An exploratory ab initio study on the conformations of ethylguanidine in its neutral [CH_3-CH_2-NH-C(=NH)NH_2] and protonated [CH_3-CH_2-NH-C(NH_2)$_2$] forms

Melody L. Mak, Salvatore J. Salpietro, R. Daniel Enriz, and Imre G. Csizmadia

Abstract: To explore the conformation intricacies of the guanidine group in the arginine side chain, ab initio computations have been carried out with ethylguanidine and the ethyl guanidinium ion. HF computations have been performed using 3–21G and 6–31G basis sets and DFT calculations were carried out at the B3LYP/6–31G(*d*) level of theory. The ethyl guanidinium ion has a single isomer due to its internal symmetry, although this structure has at least three conformations. However, several structures were found and optimized for ethylguanidine, involving the *endo*- and *exo*- orientation of the lone NH and torsional angle χ_6, as well as the torsional modes associated with χ_4 and χ_5. Torsional angle χ_5 gives rise to *s-cis* and *s-trans* structures.

Key words: ethylguanidine, ethylguanidinium ion, ab initio MO, arginine side-chain, conformational analysis.

Résumé : Dans le but d'étudier les problèmes reliés à la conformation du groupe guanidine dans la chaîne latérale de l'arginine, on a effectué des calculs ab initio sur l'éthylguanidine et l'ion éthylguanidinium. Les calculs HF ont été effectués à l'aide d'ensembles 3–21G et 6–31G alors que les calculs DFT ont été effectués au niveau B3LYP/6–31G(*d*) de la théorie. L'ion éthylguanidinium ne comporte qu'un seul isomère en raison de la symétrie interne de l'ion guanidinium même si cette structure comporte au moins trois conformations. Toutefois, on a trouvé et optimisé plusieurs structures pour l'éthylguanidine qui impliquent une orientation *endo*- et *exo*- du NH seul avec des angles de torsion χ_6 ainsi que des modes de torsion associés à χ_4 et χ_5. L'angle de torsion χ_5 conduit aux structures *s-cis* et *s-trans*.

Mots clés : éthylguanidine, ion éthylguanidinium, OM ab initio, chaîne latérale de l'arginine, analyse conformationnelle.

[Traduit par la Rédaction]

1. Introduction

Arginine is an amino acid with a positive charge at neutral pH due to its polar guanidinium group side-chain. The typical pK_a value of arginine is 12.0, the highest pK_a of all amino acids. Arginine is, therefore, important in salt bridge coupling, which is part of certain docking processes.

Arginine plays significant roles in a number of biological processes. For example, it is part of the tripeptide arginyl – glycyl – aspartic acid (RGD) which is found in adhesive proteins of extracellular matrices (1). This tripeptide serves as a cell recognition site in fibronectin. Although the cell attachment sequence is similar in different adhesive proteins, cells have the ability to distinguish them individually due to the specificity of receptors called integrins (2). Each integrin is able to recognize one RGD-containing ligand. Consequently, RGD-containing protein is extremely useful in the identification of these receptors.

Arginine is the source of nitric oxide (NO) in biological systems. NO is a free radical which serves as an intracellular second messenger and an intercellular messenger that regulates neighbouring, and possibly distant cells (3). NO takes part in many biological processes such as vasodilation, platelet aggregation, and adhesion (4–6). NO is also involved in various aspects of the central nervous system (CNS) such as the modification of pain perception, mediation of long-term potentiation and memory, controlling the cerebral blood flow, and in neurodegeneration following cerebral ischaemia (7–10). One of the two equivalent nitrogens of the terminal guanidine in L-arginine undergoes five-electron oxidation in the presence of the enzyme NO synthase (NOS), yielding NO and L-citrulline (4–6).

Current studies agree with the hypothesis that L-arginine is converted to NO by NOS in consecutive phases resulting in a multi-step mechanism (11–16). Studies by Marletta et al. (17) suggested that *N*-hydroxylation of L-arginine initiates the synthesis of NO. The discovery that the initial monooxygentation product N^G-hydroxy-L-arginine (L-NHA)

Received November 10, 1999. Published on the NRC Research Press website on May 12, 2000.

M.L. Mak, S.J. Salpietro, and I.G. Csizmadia.[1] Department of Chemistry, University of Toronto, Toronto, ON M5S 3H6, Canada.
R.D. Enriz. Departamento de Quimica, Universidad Nacional de San Luis, 5700 San Luis, Argentina.

[1]Author to whom correspondence may be addressed.
e-mail: icsizmad@chem.utoronto.ca

Scheme 1.

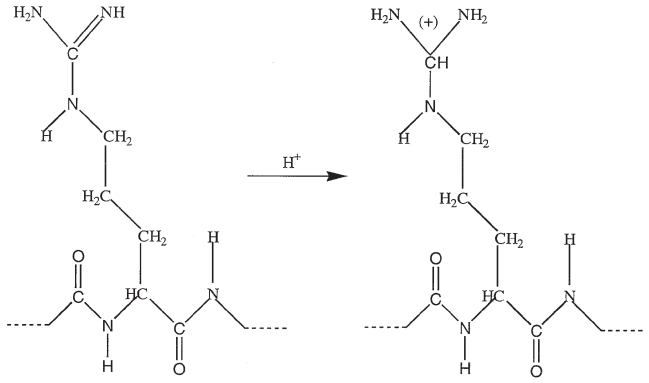

Scheme 2.

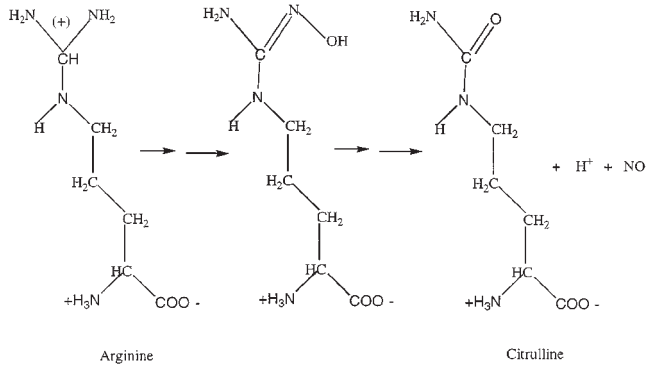

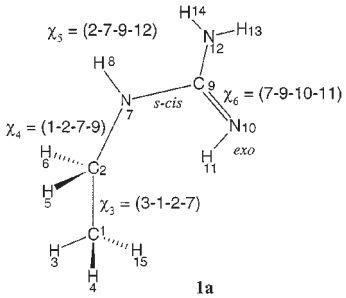

1a

Scheme 3.

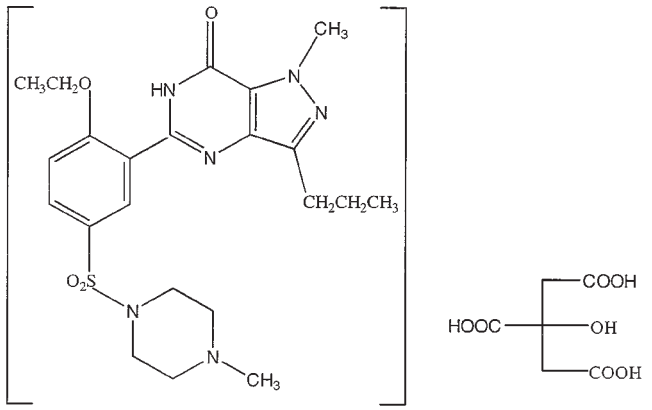

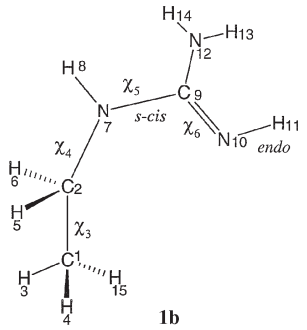

1b

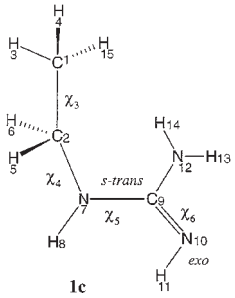

1c

is oxidized only at the guanidine nitrogen that has the hydroxyl group (16) agrees with the mechanism proposed by Marletta et al. (17). The oxidation of *N*-hydroxyguanidine, as an L-NHA model, was first studied by Fukuto et al. (13). Recently, the nitric oxide – cyclic guanosine monophosphate (cGMP) signal transduction system is regarded as an ubiquitous pathway for intra- and intercellular communication (18, 4). It was also discovered that endogeneous vasodilators, such as acetylcholine, have no direct action on the vascular smooth muscle, but act on endothelial cells. Upon the action of vasodilators, the cells release NO, which is a "labile factor" that diffuses into the overlying smooth muscles. The smooth muscles underlying the blood vessel walls are relaxed by NO which spreads by diffusion (18, 3–6, 19*a*). For example, the release of NO by the cavernous nerves, which induces the relaxation of smooth muscles in the corpus cavernosum during sexual stimulation, has prompted the recent development of sildenafil citrate, or VIAGRA®, in treatment of erectile dysfunction.

N-methyl guanidine has been used as a model compound for arginine to study the mechanism of NO release using ab initio molecular computations (19*b*).

Previous work has already been done regarding the conformations of simple amino acids such as glycine and alanine (20). Other amino acids with more complicated side chains, such as phenylalanine (Phe) (21), serine (Ser) (22–24), cysteine (Cys) (footnote 2), selenocysteine (Sec) (25), aspartic acid (Asp) (26), and asparagine (Asn) (27) have also been studied. With the exception of proline (Pro) (28), all 19 chiral amino acids are expected to have nine different backbone conformations.

Ethylguanidine (**1**) and ethylguanidinium ion (**2**) are the terminal portions of the side chain (R-group) of the arginine

[2] M.A. Zamora, H.A. Baldoni, A.M. Rodriguez, R.D. Enriz, C.P. Sosa, A. Perczel, A. Kucsman, Ö. Farkas, E. Deretey, J.C. Vank, and I.G. Csizmadia. J. Am. Chem. Soc. (in preparation).

Scheme 4.

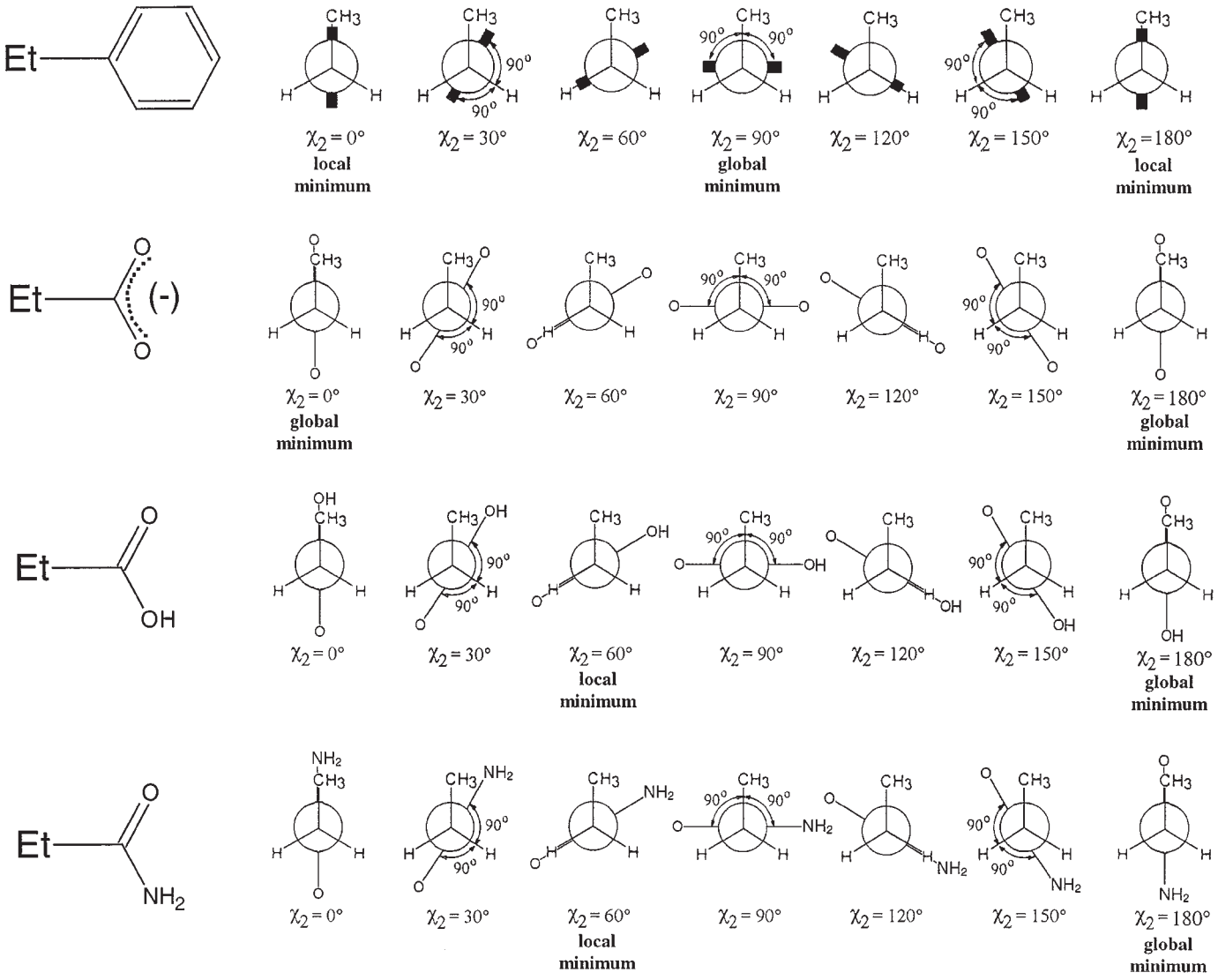

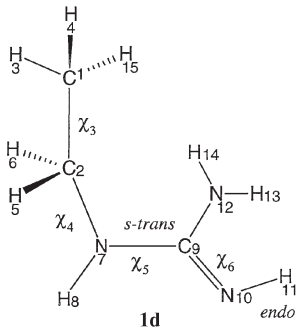

1d

residue in *N*-formyl-argininamide (**3**) and its side chain terminal *N*-protonated form (**4**), respectively. Arginine can be divided into two portions: the backbone, which is analogous to glycine (or alanine), and the side chain, which is an alkyl guanidine.

Due to the large number of conformations of the amino acid side chain, even if it is of a modest size, it is simply not practical to optimize the entire structure before we have a preliminary knowledge about the intricacy of its conformations. As an appropriate model one may study **1** instead of **3** or, in a similar fashion, **2** in order to better understand the behavior of **4**.

The two torsional modes of motion (rotation about the C—C and C—N bonds) are labeled as χ_3 and χ_4 respectively in all four structures (**1**–**4**) even though structures **1** and **2** have no χ_1 and χ_2 torsional modes.

2. Computational methods

Quantum chemical calculations involving geometry optimizations were carried out using the Gaussian 94 program at the Hartree Fock (HF) and DFT levels of theory using various basis sets. The following two basis sets have been employed for HF calculations: 3–21G and 6–31G. Geometries optimized at the HF level were subjected to further geometry optimization using DFT calculation at the B3LYP/6–31G(*d*) level of theory. Points calculated by the 1D-scan for the $E = E(\chi_4)$ potential energy curve (PEC) of

Fig. 1. Potential energy curve $E = E(\chi_2)$ of ethylbenzene (top) and that of propionate ion (bottom) both calculated at HF/3-21G.

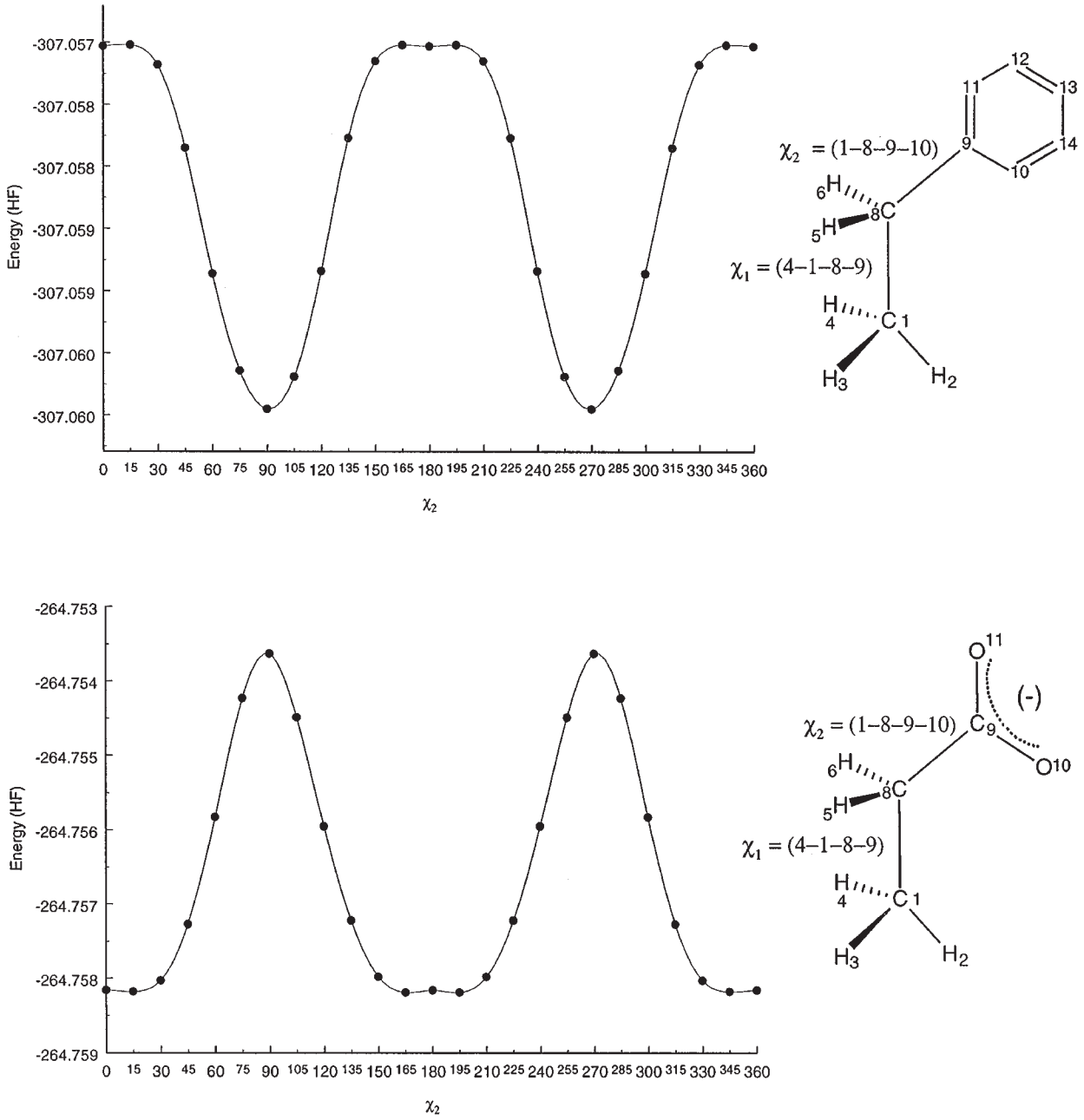

1a was obtained at the HF/6–31G level of theory and the $E = E(\chi_5)$ PEC of **2** was obtained at the HF/3–21G level of theory. Surface points generated by 2D–PES scans were calculated at HF/3–21G level of theory. All curves and surface points obtained were plotted using the Axum 5.0c program.

3. Results and discussion

When a planar moiety is twisted about a single bond with respect to a tetrahedral moiety, in principle six minima may appear. Some of these conformations are shown schematically in Scheme 4. In all cases shown, the methyl group was staggered (i.e., $\chi_1 = 60°$). For the case of ethyl benzene (29) only two unique minima were shown to exist; one at $\chi_2 = 0°$ (the plane of the phenyl ring eclipsed with the C—C bond) and the other one at $\chi_2 = 90°$ (the plane of the phenyl ring being perpendicular to the C—C bond). The global minimum was found to be the one in which the planar moiety was perpendicular to the C—C bond ($\chi_2 = 90°$). Of course, both of these minima occurred twice in full 360° rotation due to the fact that the two sides of the benzene ring were identical. The potential energy curve of the other symmetrical compound, namely the propionate ion, is the exact mirror image of that associated with ethyl benzene, where the minimum of one is the maximum of the other (Fig. 1). The two asymmetrical compounds, propionic acid and

Fig. 2. Potential energy curve $E = E(\chi_2)$ of propionic acid (top) and that of propionamide ion (bottom) both calculated at HF/3-21G.

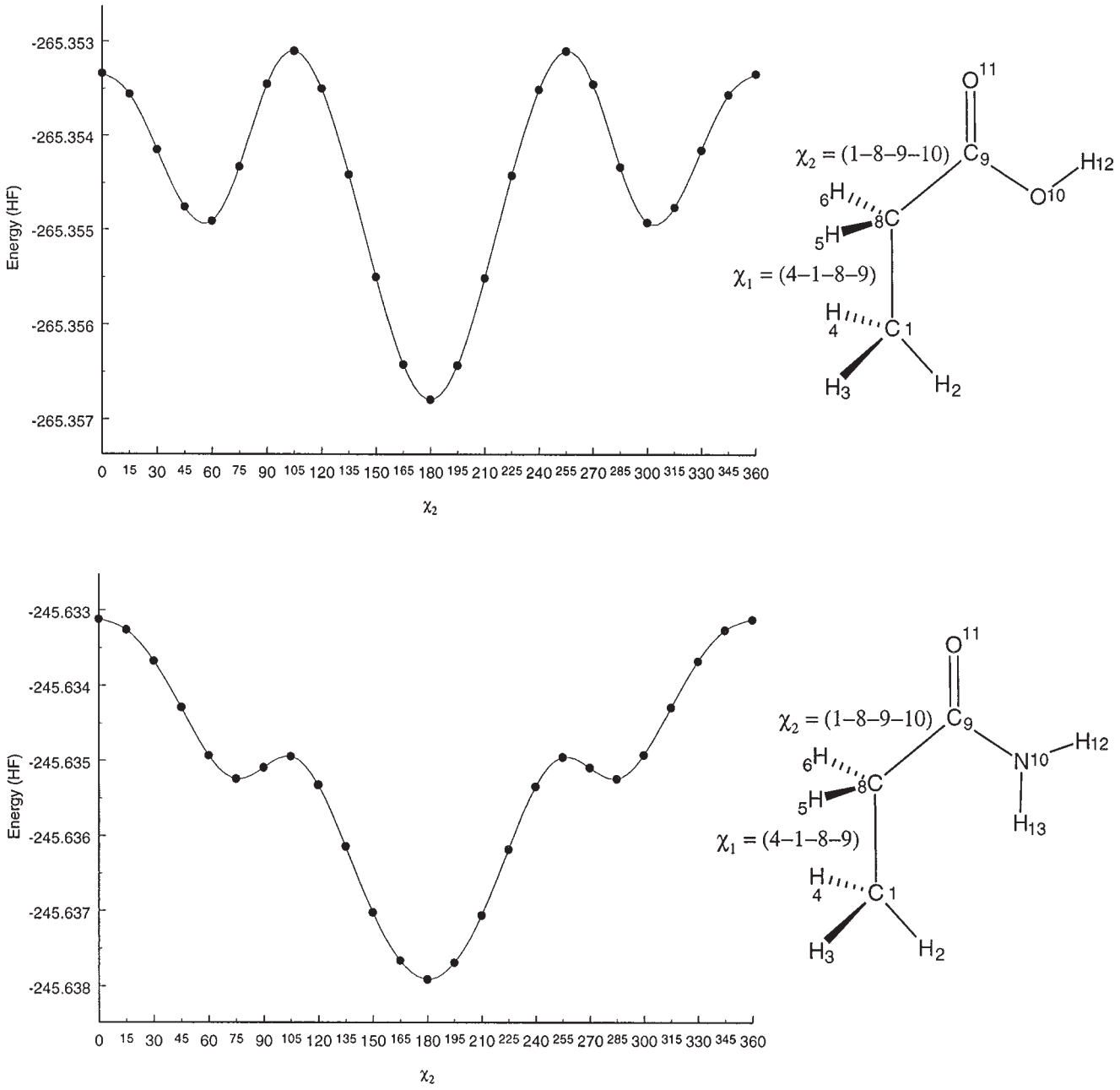

propionamide, give rise to a global minimum when they are in the *anti* conformation and local minima in the *gauche* conformations. (Fig. 2)

In the case of ethylguanidine (**1**) and the ethylguanidinium ion (**2**), there are two torsional angles χ_3 and χ_4. The dihedral numbering is in accord with the amino acid convention (corresponding to χ_1 and χ_2 in ethylbenzene). These are two kinds of bonds, C—C and C—N, with respect to which the guanidine group could be either eclipsed or perpendicular.

3.1 Energetic considerations

3.1.1 Ethylguanidine

Figure 3 shows the torsional potential, with varying χ_4, for ethylguanidine in its *s-cis*/*exo* **1a** structure calculated using the HF/6–31G level of theory. The global minimum occurs at 180° (the *anti* form). For all four structures (**1a**, **1b**, **1c**, and **1d**) g^+, a, and g^- were shown to have energy minima. We optimized these minima using three levels of theory (Hartree Fock 3–21G, 6–31 G, and DFT/B3LYP). The results are summarized in Table 1.

The ethyl rotation as characterized by the PES of the type $E = E(\chi_3, \chi_4)$ for the structures **1a**, **1b**, **1c**, and **1d** are presented in Figs. 4, 5, 6, and 7 respectively. Although the four surfaces are noticeably different, the three-fold periodicity of the CH_3 rotation (along χ_3) is fully apparent. The relative stabilities of these $4 \times 3 = 12$ structures are illustrated in Fig. 8. One can observe that the *gauche* conformation of **1b** is the global minimum, and that its *anti* conformation is of a relatively low energy comparing to the other three *anti*

Table 1. Optimized torsional angle (χ_4) and energy values of the conformational minima ($\lambda = 0$) of structures **1a**, **1b**, **1c**, and **1d** using various basis sets at the HF and DFT level of theory.

Structure	Basis set	Optimized Parameters			
		(χ_4)	E_{min} (hartree)	ΔE (kcal/mol)	$\Delta\Delta E$ (kcal/mol)
1a	HF/3–21G	82.27	–280.6102467	1.35	0.09
		168.67	–280.6101103	1.44	0.00
		–74.59	–280.6098721	1.59	0.15
	HF/6–31G	78.29	–282.0620464	0.92	0.44
		171.21	–282.0627458	0.49	0.00
		–78.22	–282.0620465	0.92	0.44
	B3LYP/6–31G(d)	75.48	–283.9874326	0.10	0.30
		177.36	–283.9879119	0.40	0.00
		–81.42	–283.9865861	0.43	0.83
1b	HF/3–21G	79.38	–280.6124011	0.00	0.97
		162.46	–280.6108520	0.97	0.00
		–79.41	–280.6124010	0.00	0.97
	HF/6–31G	84.26	–282.0635187	0.00	3.98
		168.25	–282.0630562	0.29	0.00
		–84.12	–282.0635189	0.00	0.29
	B3LYP/6–31G(d)	76.14	–283.9877135	0.27	0.27
		173.42	–283.987277	0.00	0.00
		–76.27	–283.9877134	0.27	0.27
1c	HF/3–21G	100.76	–280.6079228	2.81	0.06
		157.14	–280.607826	2.87	0.00
		–64.80	–280.6085254	2.43	0.44
	HF/6–31G	75.57	–282.0599067	2.27	0.39
		–179.98	–282.060534	1.87	0.00
		–85.42	–282.0598876	2.28	0.41
	B3LYP/6–31G(d)	67.85	–283.9857075	0.98	0.43
		179.73	–283.9850151	1.42	0.00
		–67.97	–283.9857073	0.99	0.43
1d	HF/3–21G	63.05	–280.6087256	2.31	0.44
		189.70	–280.6080244	2.75	0.00
		–62.95	–280.6087256	2.31	0.44
	HF/6–31G	77.53	–282.0603108	2.01	0.41
		–179.94	–282.0609655	1.60	0.00
		–77.30	–282.0603107	2.01	0.41
	B3LYP/6–31G(d)	65.46	–283.9856017	1.05	3.17
		179.94	–283.9805551	4.22	0.00
		–65.66	–283.9856012	1.05	3.17

Fig. 3. Potential energy curve $E = E(\chi_4)$ of structure **1a** calculated at HF/6-31G.

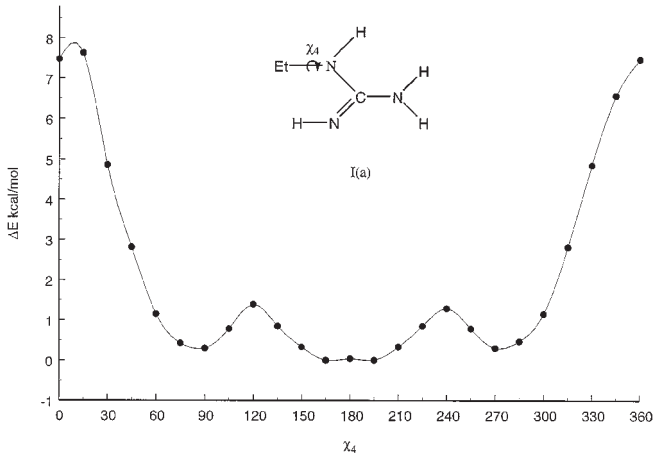

forms. The *anti* conformation of **1d** is highest in energy. It is also interesting to note that the energy difference between the *anti* and *gauche* forms of **1d** is the greatest, whereas this energetic difference is the smallest in **1b**.

3.1.2 Ethylguanidinium ion

The protonated form of the ethylguanidine (**1**) is the ethyl guanidinium ion (**2**). Due to the internal symmetry of the N-$C(NH_2)_2^+$ moiety, this species has only one arrangement, unlike **1** which has four: **1a**, **1b**, **1c**, and **1d**. Consequently, only the ethyl rotation $E = E(\chi_3, \chi_4)$ is important, of which the 1D cross-section $E = E(\chi_4)$ predominates. The energy values for the 1D-scan are computed at the HF/3–21G level of theory. This PEC is depicted in Fig. 9. The $E = E(\chi_3, \chi_4)$ PES is depicted in Fig. 10. The PEC has a pattern similar to those seen in Fig. 2. Another PEC cross-section of the PEHS $E = E(\chi_5)$ is of particular interest since it interconnects the *s-cis* and *s-trans* conformers. However, in the case of the

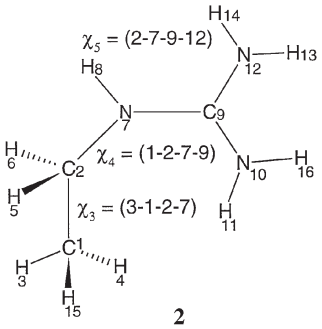

2

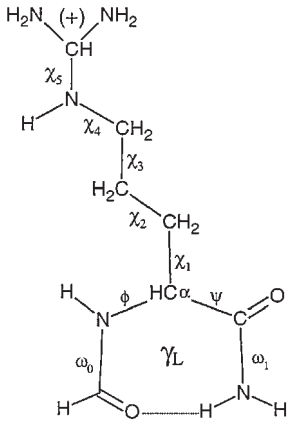

3

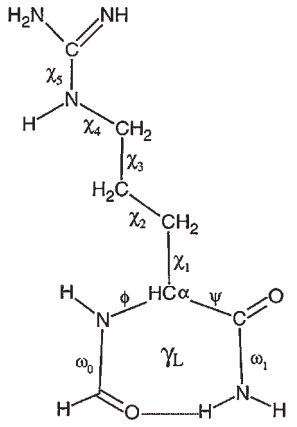

4

protonated form they become degenerate as shown in Fig. 11. It is interesting to note that the curve (Fig. 11) is analogous to that of Et-COO(-) of Fig. 1. The principal results of the geometry optimizations achieved at these levels of theory are summarized in Table 2.

For the proton affinity (PA) we may recognize that a number of values may be calculated. There is only one PEC for the protonated form (**2**) but there are four PECs for (**1**). Two vertical proton affinity values may be identified using these PECs. The two vertical ones involve g→g and a→a. These values are summarized in Table 3.

Table 2. Optimized torsional angles (χ_4) and energy values of the conformational minima ($\lambda = 0$) of structure **2** CH_3-CH_2-NH-$C(NH_2)_2$ using various basis sets at the HF and DFT level of theory.

Basis set	Optimized Parameters		
	(χ_4)	E_{min} (hartree)	ΔE (kcal/mol)
3–21G	81.79	–281.0413070	0.61
	179.52	–281.0422726	0
	–82.59	–281.0413097	0.60
6–31G	85.00	–282.4864891	0.91
	179.98	–282.4879377	0
	–85.06	–282.4864888	0.91
B3LYP/6–31G(d)	90.52	–284.3914612	0.37
	179.94	–284.3920511	0
	–90.54	–284.3914611	0.37

Table 3. Proton affinities (in kcal/mol) for the 3 conformational minima of structures **1a**, **1b**, **1c,** and **1d** at HF/6–31G and B3LYP/6–31G(*d*) levels of theory.

Conformation	Base	HF/6–31G	B3LYP/6–31G(d)
g^+	**1a**	266.34	253.53
	1b	265.42	253.36
	1c	267.70	254.61
	1d	267.43	254.68
a	**1a**	266.81	253.60
	1b	266.62	254.00
	1c	268.20	255.42
	1d	267.93	258.22
g^-	**1a**	266.34	254.43
	1b	265.42	253.36
	1c	267.69	254.61
	1d	267.43	254.68

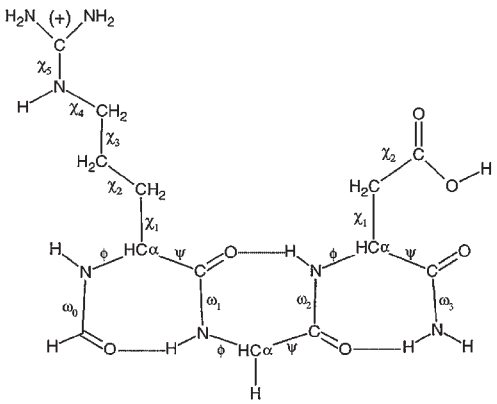

5

The first ab initio proton affinities were computed in Toronto (30) in 1968. A collection of relative proton affinities was compiled by Lias et al. (31) in 1984. In 1993, Radom (32) provided state-of-the-art calculation of various proton affinities, some of which involved saturated nitrogen compounds. Note that the present proton affinities are generated for illustrative purposes only and not for state of the art

Fig. 4. Conformational potential energy surface $E = E(\chi_3, \chi_4)$ of structure **1a** as landscape (top) and projected contour plot (bottom) calculated at HF/3-21G.

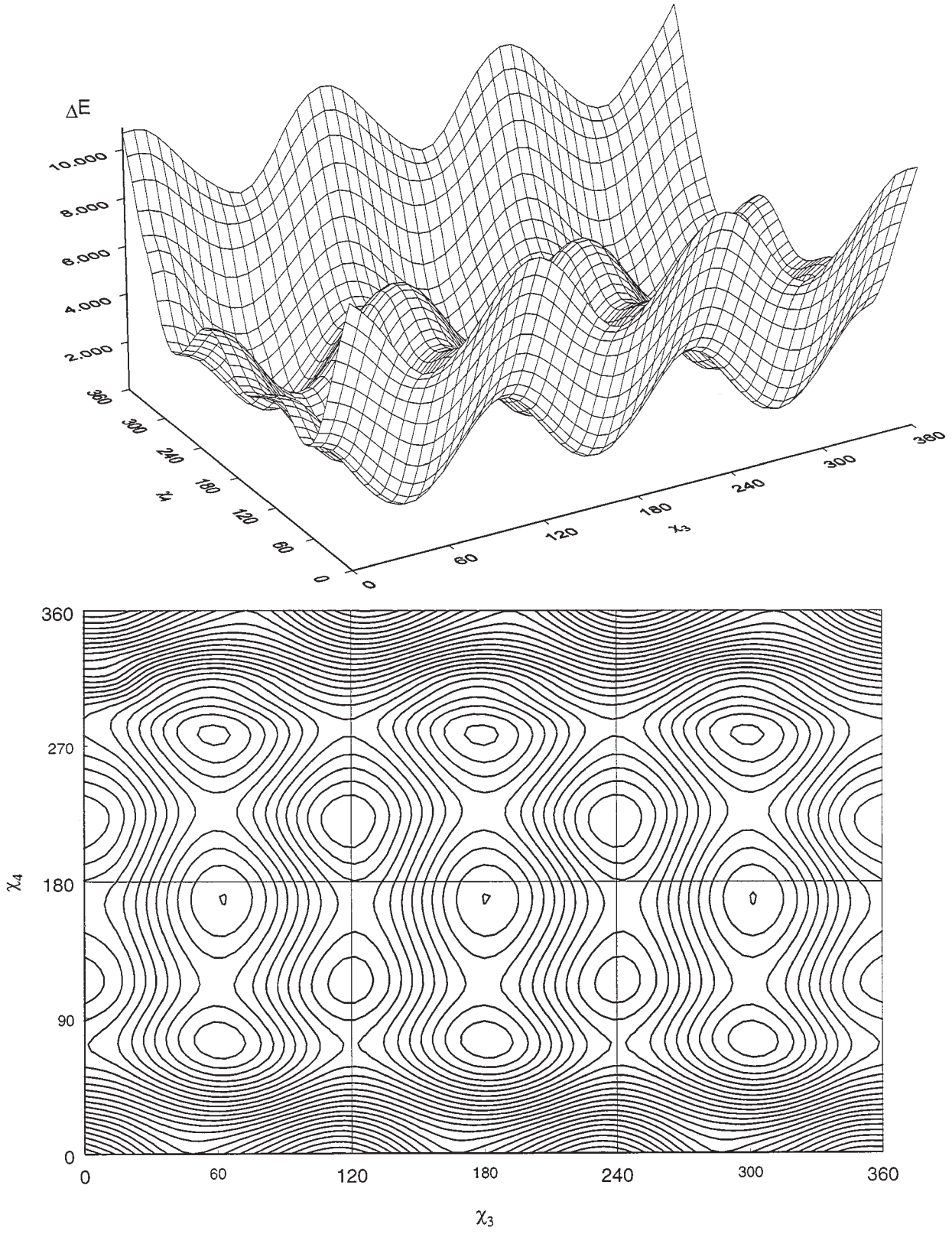

Fig. 5. Conformational potential energy surface landscape (top) $E = E\chi_3, \chi_4)$ of structure **1b** and projected contour plot (bottom) calculated at HF/3-21G.

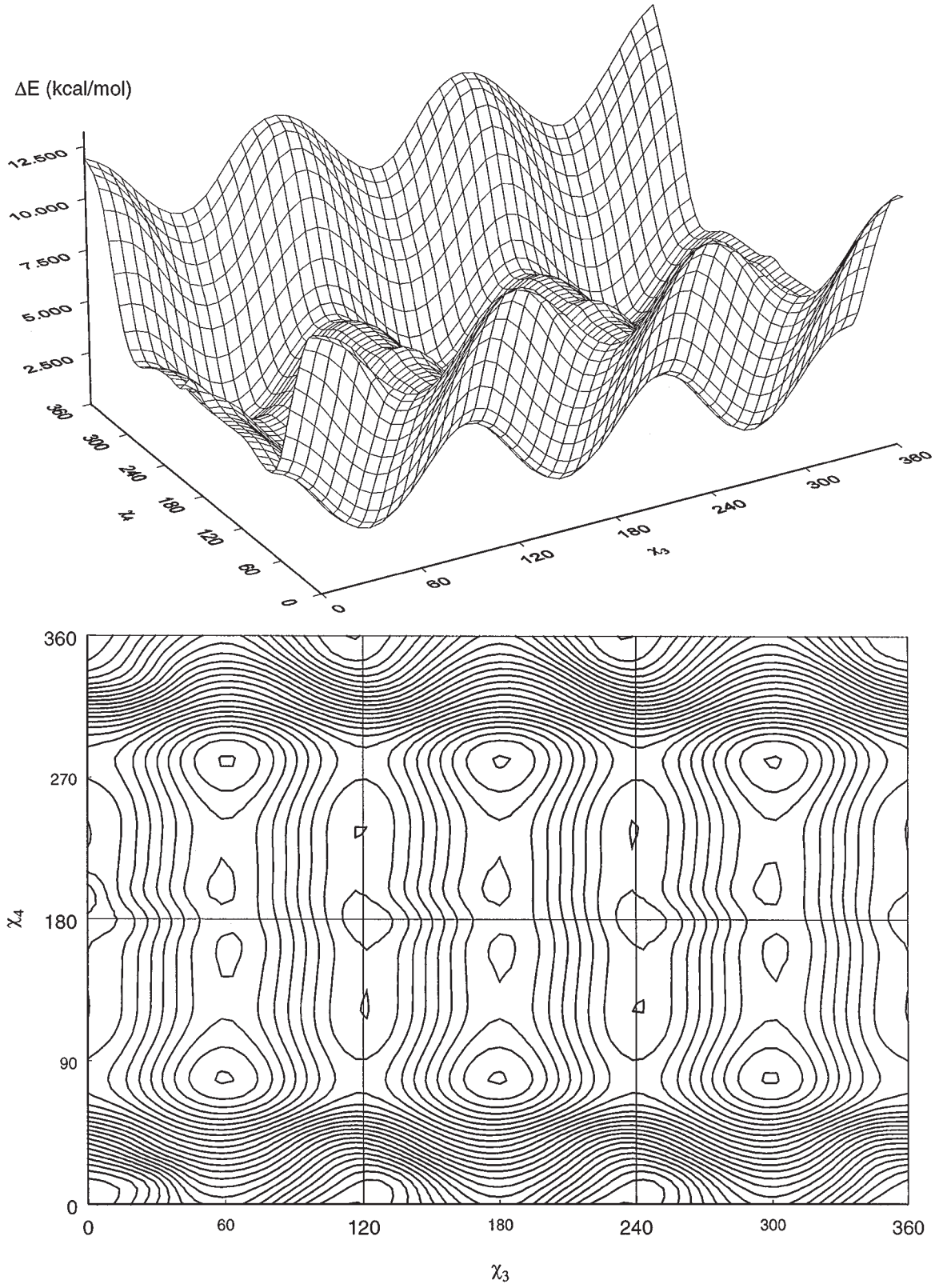

Fig. 6. Conformational potential energy surface landscape (top) $E = E(\chi_3, \chi_4)$ of structure **1c** and projected contour plot (bottom) calculated at HF/3-21G.

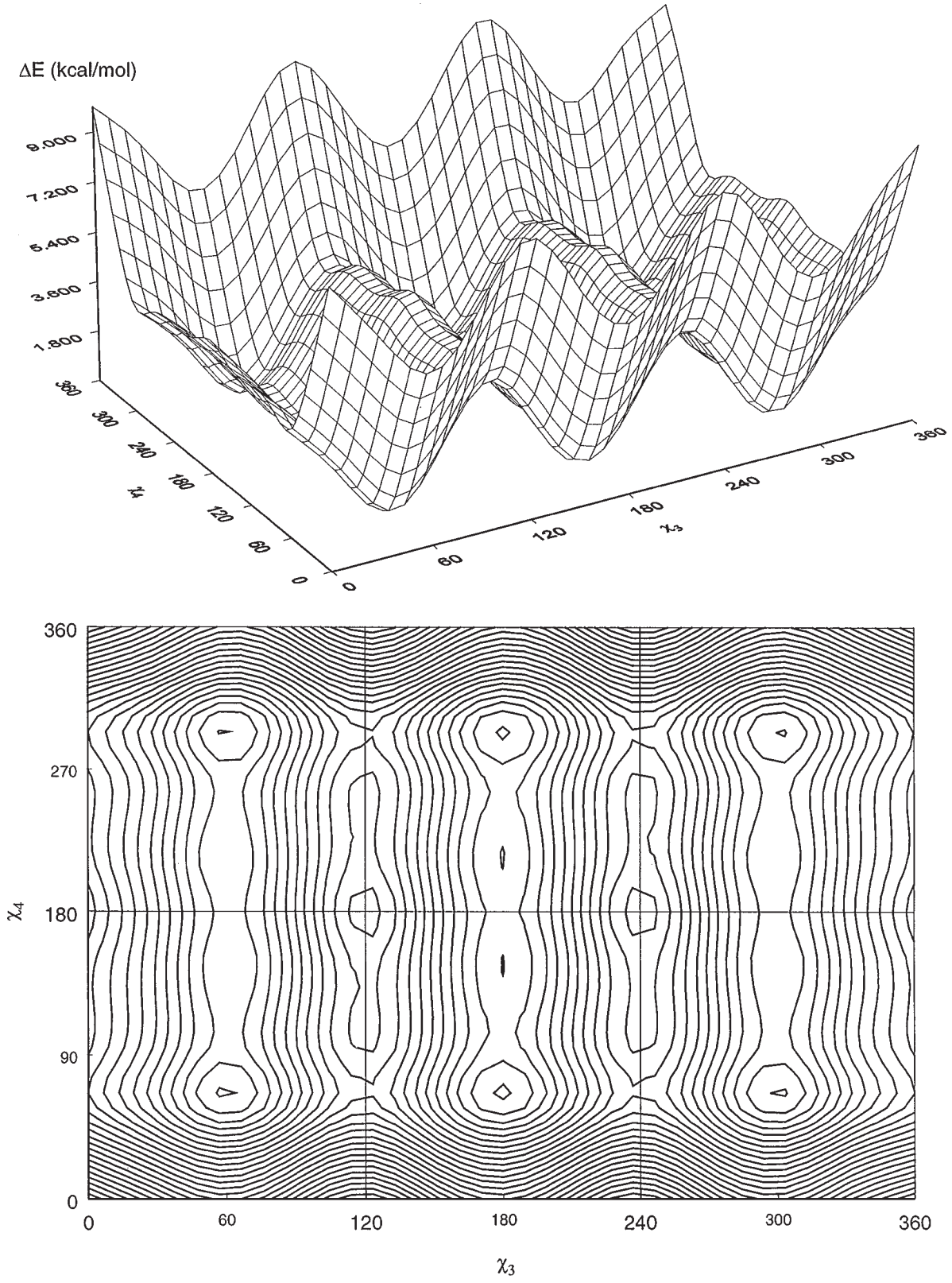

Fig. 7. Conformational potential energy surface landscape (top) $E = E(\chi_3, \chi_4)$ of structure **1d** and projected contour plot (bottom) calculated at HF/3-21G.

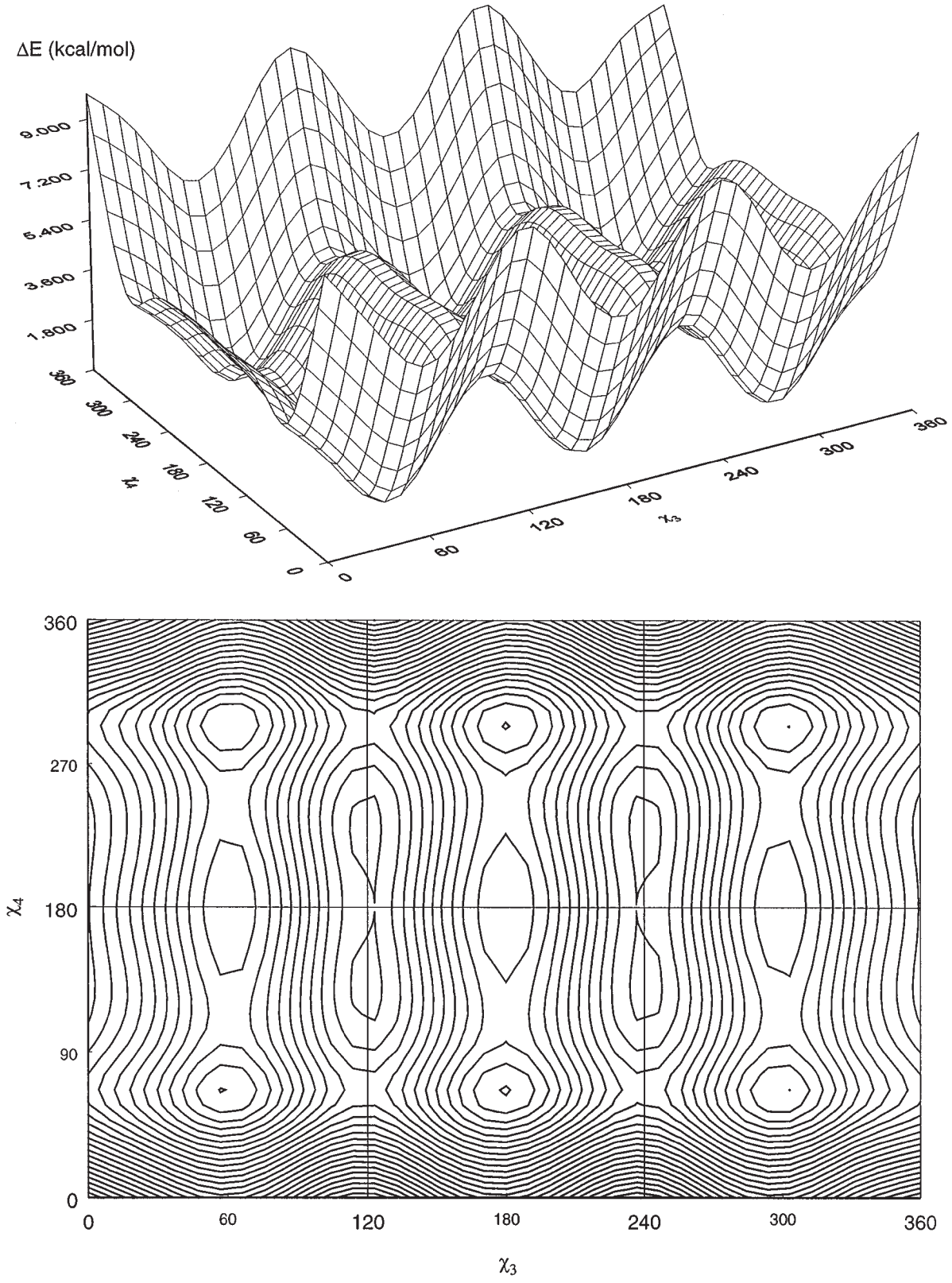

Fig. 8. Topological representation of the $E = E(\chi_4, \chi_5, \chi_6)$ Potential energy hypersurface for compound **1**. Energy differences were computed at the B3LYP/6-31G(*d*) level of theory.

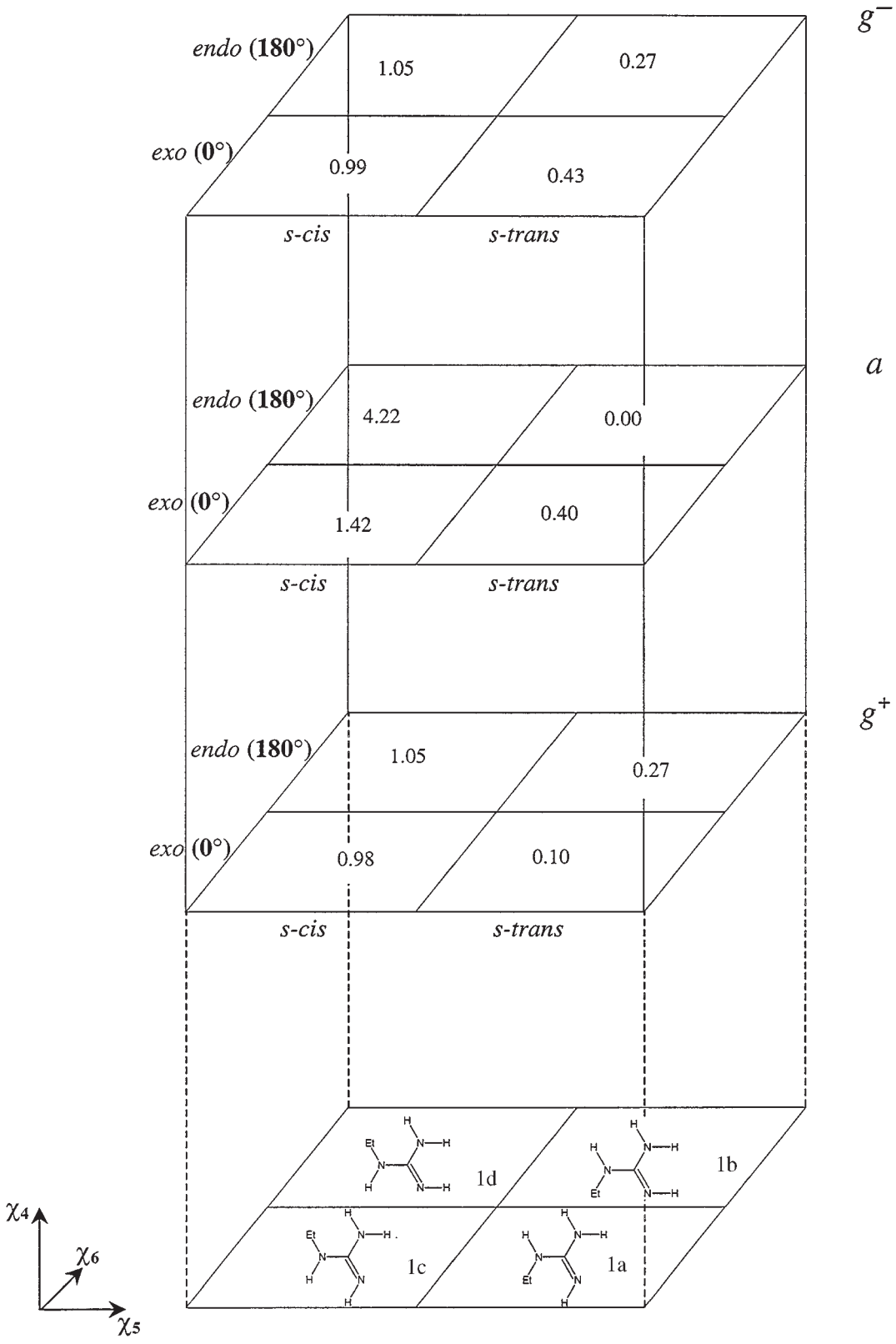

Fig. 10. Conformational potential energy surface landscape (top) $E = E(\chi_3, \chi_4)$ of structure **2** and projected contour plot (bottom) calculated at HF/3-21G.

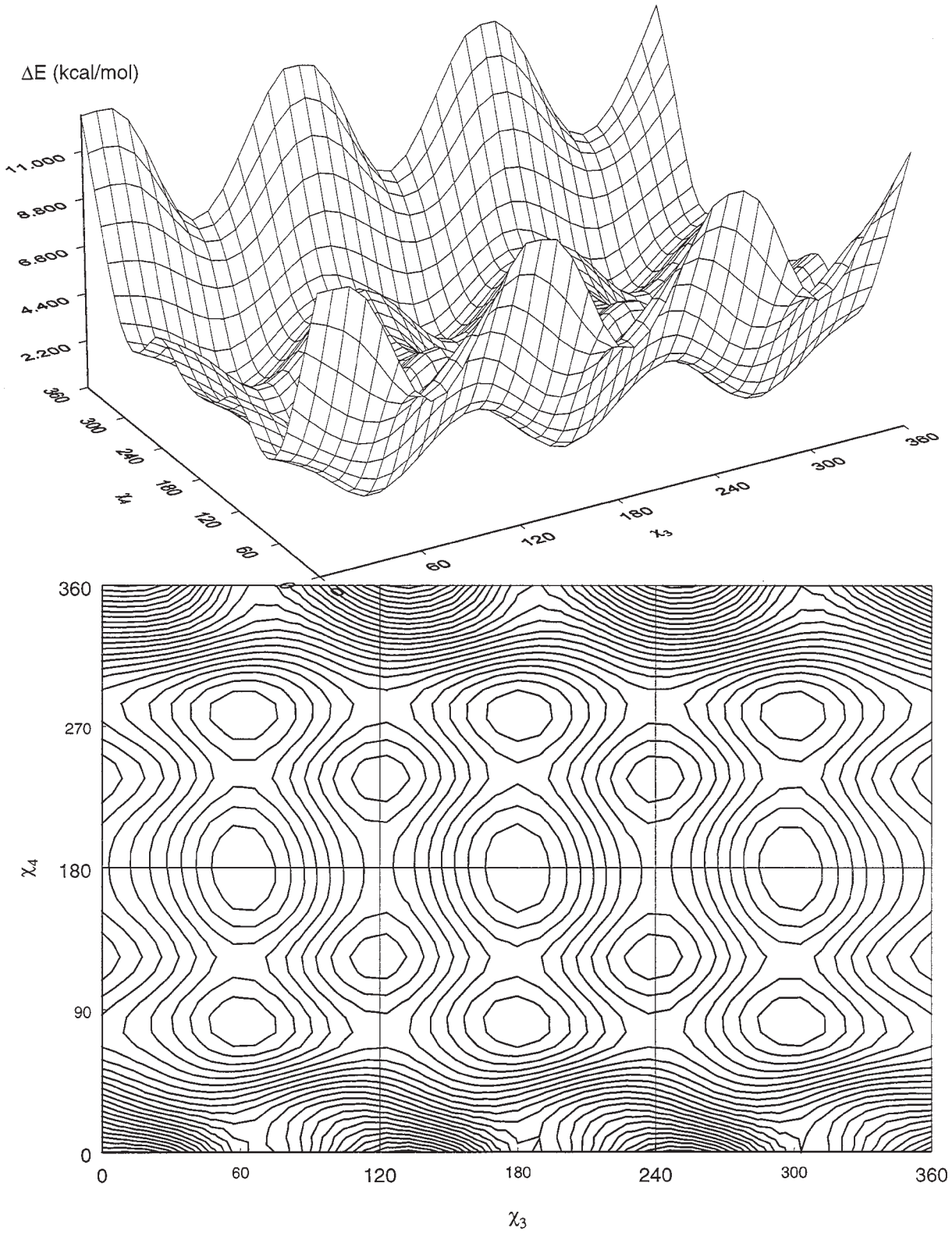

Fig. 9. Potential energy curve $E = E(\chi_4)$ of structure **2** calculated at HF/3-21G.

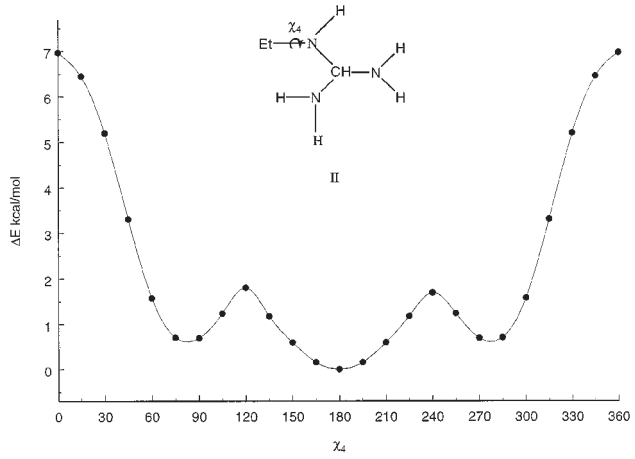

Fig. 11. Potential energy curve $E = E(\chi_5)$ of structure **2** calculated at HF/3-21G.

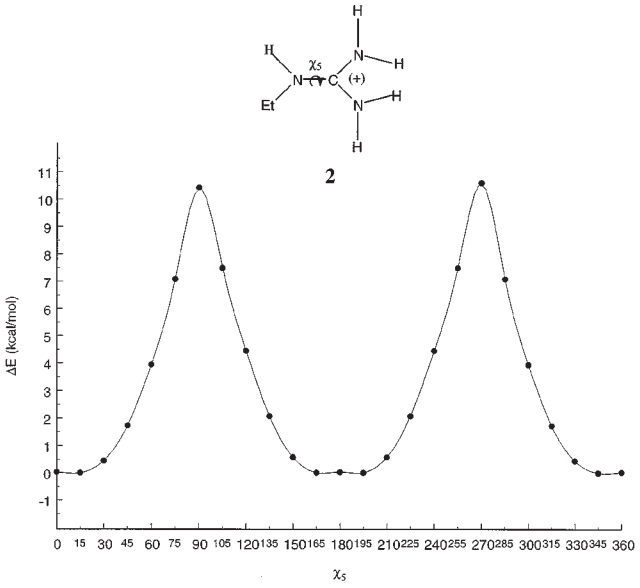

accuracy. It is worthy to mention, however, that at least the trend in proton affinities is apparent when one compares the values at the HF level with those of the DFT level of theory. These values are to show that different conformations give different proton affinities. Proton affinity is defined with a positive sign and is actually the deprotonation energy of the conjugated acid. The a→a and the g→g vertical deprotonation energies are shown in Fig. 12 and Fig. 13 respectively. In this way, one can determine the order of relative acidities of the four protons in the guanidinium ion (Fig. 14).

Proton affinities of amino acids are studied in detail (33) and the deprotonation of side chain protonated arginine (34) has also been investigated. It has also been pointed out that the proton at the first N—H bond of side chain-protonated

Fig. 12. Vertical proton affinity values for the transition a→a calculated at HF/6-31G.

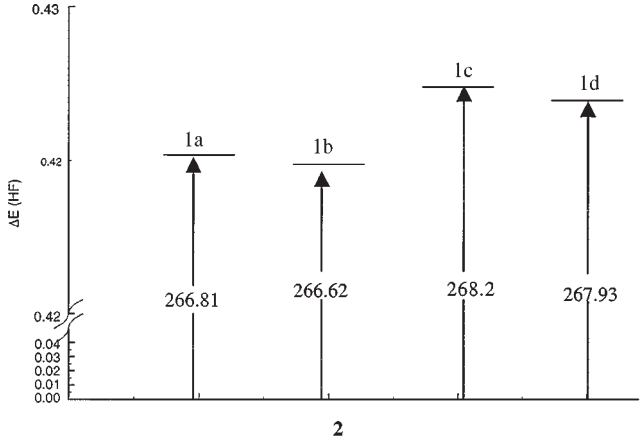

Fig. 13. Vertical proton affinity values for the transition g→g calculated at HF/6-31G.

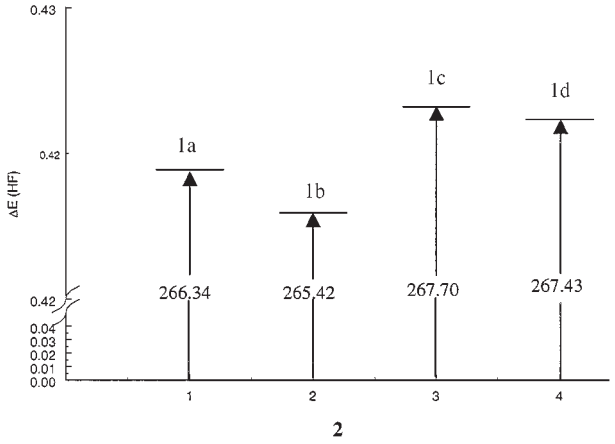

arginine (N^7—H^8 in **2**) can also deprotonate if the lone pair formed in the deprotonation is stabilized by backbone→side chain hydrogen bonding. Other reactions of the arginine side chain have also been investigated (19*b*, 35) recently.

3.2 Geometrical considerations

For the ease of identification of the various geometrical parameters, the symbolic *z*-matrix is given in Table 4. Tables 5, 6, 7, and 8 (Supplementary material)[3] summarize optimized geometrical parameters for **1a**, **1b**, **1c**, and **1d**. It may be interesting to compare how some parameters remain virtually unchanged with conformational variation while others vary noticeably.

Table 9 (Supplementary material)[3] gives the geometrical parameters for **2**. It is noteworthy to compare what happens to the C=N double bond of **1**, upon protonation, leading to ethylguanidinium ion (**2**).

3.2.1 Ethylguanidine

Ethylguanidine has four stereoisomeric forms, as shown in Fig. 8; they are *s-cis*/*endo*, *s-cis*/*exo*, *s-tran*/*endo*, and

[3] Supplementary material may be purchased from: The Depository of Unpublished Data, Document Delivery, CISTI, National Research Council Canada, Ottawa, Ontario, Canada, K1A 0S2.

Fig. 14. Hierarchy of acidity of the four protons of ethylguanidium ion.

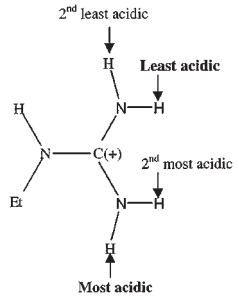

s-trans/*exo*. The *cis–trans* relationship is assigned with respect to the orientation of the ethyl moiety around the torsional angle χ_5, and the *exo–endo* relationship is assigned according to the orientation of the hydrogen double bonded to the nitrogen (N^{10}=H^{11}). If the hydrogen is pointing out of plane, the isomer is assigned *exo*, with χ_6 = 180°; similarly, if the hydrogen is pointing towards the plane, the isomer is assigned *endo*, χ_6 = 0°. One can compare C^9=N^{10} (B9) and C^9—N^{12} (B11) bond lengths of **1** with the C—N bond lengths of **2**, and deduce the extent of the double bond nature. The C^9—N^{12} and C^9—N^{10} bond lengths (1.340) of **2** are between the lengths of the C^9=N^{10} bond and the C^9—N^{12} bond of **1**. The difference between these two bond lengths is the greatest in all three conformations of **1c**. So, the single bonds C^9—N^{10} and C^9—N^{12} of **2** have more "double bond" character than the single bond C^9—N^{12} of **1**.

3.2.2 Ethylguanidinium ion

While the guanidinium ion is symmetrical, ethylguanidinium is not. Presence of the ethyl moiety makes all five hydrogens of guanidinium ion inequivalent. The four hydrogens for deprotonation can lead to four isomers of the neutral ethylguanidine.

The lengths of N—H bonds of the guanidino end are identical, indicating that the positive charge is delocalized. It is also worth noting that N_{10}—H_{11} (B10) of **2** is the shortest of the four NH_2 hydrogens although H_{11} is the most acidic of the four (Fig. 14). Therefore, the N—H bond length is not governed by acidity (i.e., electronic effects), but rather by the orientation of the ethyl moiety (i.e., steric effects). N^{10}—H^{11} is *syn* with respect to the ethyl group and is therefore sterically the closest to the aliphatic group.

4. Acknowledgements

The continuous financial support of the Natural Sciences and Engineering Research Council (NSERC) of Canada is gratefully acknowledged. We would also like to thank the NCI for the use of services at Frederick Biomedical Supercomputing Center.

References

1. E. Ruoslahti and M.D. Pierschbacher. Science (Washington, D.C.), **238**, 491 (1987).
2. R.O. Hynes. Cell (Cambridge, Mass.), **48**, 549 (1987).
3. P.K. Moore and R.L.C. Handy. Trends Pharmacol. Sci. **18**, 204 (1997).
4. F. Murad, B.A. Weissman, A. Allon, and S. Shapira (*Editors*). Biochemical, pharmacological and clinical aspects of nitric oxide. Plenum Press, New York. 1995. pp. 1–11.
5. M.A. Marletta. J. Biol. Chem. **268** (17), 12231 (1993).
6. A.R. Butler, F.W. Flitney, and D.L.H. Williams. Trends Pharmacol. Sci. **16**, 18 (1995).
7. M.D. Black, E.K. Matthews, and P.P.A. Humphrey. Neuropharmacology, **33** (11), 1357 (1997).
8. Chol Lipton, Lei Pan, Sucher Chen, Singel Loscalzo, Stamler. Nature (London), **364**, 626 (1993).
9. V.L. Dawson, T.M. Dawson, E.D. London, D.S. Bredt, and S.H. Snyder. Proc. Natl. Acad. Sci. U.S.A. **88**, 6368 (1991).
10. W. Wutian and L. Linxi. Neurosc. Lett. **153**, 121 (1993).
11. J.F. Kerwin and M. Heller. Med. Res. Rev. **14**, 23 (1994).
12. N.M. Olken and M.A. Marletta. Biochemistry, **32**, 9677 (1993).
13. J.M. Fukuta, D.J. Stuehr, and P.L. Feldman. J. Med. Chem. **36**, 2666 (1993).
14. J.S. Valentine, J.N. Burstyn, and L.D. Margernum. *In* Oxygen complexes and oxygen activation by transition metals. *Edited by* A.E. Martell, D.T. Martella, and D.T. Sawyer. Plenum Press, New York. 1988. pp. 175–187.
15. D.J. Stuehr, N.S. Kwon, C.F. Nathan, O.W. Griffith, P.L. Feldman, and J. Wiseman. J. Biol. Chem. **266**, 6259 (1991).
16. D.J. Stuehr and O.W. Griffith. Adv. Enzymol. Relat. Areas Mol. Biol. 297 (1992).
17. M.A. Marletta, P.S. Yoon, R. Ivengar, C.D. Leaf, and J.S. Wishnok. Biochemistry, **27**, 8706 (1988).
18. T. Dalkara and M.A. Moskowitz. *In* Biochemical, pharmacological and clinical aspects of nitric oxide. *Edited by* B.A. Weissma, A. Allon, and S. Shapira. Plenum Press, New York. 1995. pp. 189–194.
19. (*a*) S. Moncada, R.M.J. Palmer, and E.A. Higgs. Pharmacol. Rev. **43**, 109 (1991); (*b*) M.B. Santillan, G.M. Ciuffo, E.A. Jauregui, and I.G. Csizmadia. THEOCHEM, **468**, 223 (1999).
20. (*a*) A. Perczel, J.G. Angyan, M. Kajtar, W. Viviani, J.L. Rivail, J.F. Marcoccia, and I.G. Csizmadia. J. Am. Chem. Soc. **113**, 6256 (1991); (*b*) M.A. McAllister, A. Perczel, P. Császár, W. Viviani, J.L. Rivail, and I.G. Csizmadia. THEOCHEM, **288**, 161 (1993).
21. (*a*) Ö. Farkas, M.A. McAllister, J.H. Ma, M. Hollósi, and I.G. Csizmadia. THEOCHEM, **369**, 105 (1996); (*b*) A. Perczel, Ö. Farkas, and I.G. Csizmadia. Can. J. Chem. **75,** 1120 (1997); (*c*) I. Jakli, A. Perczel, Ö. Farkas, M. Hollosi, and I.G. Csizmadia. THEOCHEM, **455**, 303 (1998).
22. (*a*) Ö. Farkas, J.F. Marcoccia, M. Hollósi, and I.G. Csizmadia. THEOCHEM, **331**, 27 (1995); (*b*) A. Perczel, Ö. Farkas, and I.G. Csizmadia. J. Comput. Chem. **17**, 821 (1996).
23. A. Perczel, Ö. Farkas, and I.G. Csizmadia. J. Am. Chem. Soc. **118**, 7809 (1996).
24. A. Perczel, Ö. Farkas, and I.G. Csizmadia. THEOCHEM, **455**, 303 (1998).
25. J.C. Vank, C.P. Sosa, A. Perczel, and I.G. Csizmadia. Can. J. Chem. **78**, 395 (2000).
26. S.J. Salpietro, A. Perczel, Ö. Farkas, R.D. Enriz, and I.G. Csizmadia. THEOCHEM, **497**, 37 (2000).
27. M. Berg, S.J. Salpietro, and I.G. Csizmadia. THEOCHEM, (in press).
28. H.A. Baldoni, A.M. Rodriguez, M.A. Zamora, G.N. Zamarbide, R.D. Enriz, Ö. Farkas, P. Csaszar, L.L. Torday, C.P. Sosa, I. Jakli, A. Perczel, J.G. Papp, M. Hollosi, and I.G. Csizmadia. THEOCHEM, **465**, 79 (1999).
29. Ö. Farkas, S.J. Salpietro, P. Csaszar, and I.G. Csizmadia. THEOCHEM, **367**, 25 (1996).

30. A.C. Hopkinson, N.K. Holbrook, K. Yates, and I.G. Csizmadia. J. Chem. Phys. **49**, 3596 (1968).
31. S.G. Lias, J.F. Liebman, and R.D. Levin. J. Phys. Chem. Ref. Data, **13**, 695 (1984).
32. B.J. Smith and L. Radom. J. Am. Chem. Soc. **115**, 4885 (1993).
33. Z.B. Maksic and B. Kovacevic. Chem. Phys. Lett. **307**, 497 (1999).
34. Z.B. Maksic and B. Kovacevic. J. Chem. Soc. Perkin Trans. 2, 2926 (1999).
35. C. Kozmutza, E.M. Evleth, L. Udvardi, and J. Pipek. Acta Biol. Hung. **49**, 219 (1998).